MRI-Compatible Optically-Sensed Cello

Avrum D. Hollinger and Marcelo M. Wanderley
Input Devices and Music Interaction Laboratory (IDMIL)
Centre for Interdisciplinary Research in Music Media and Technology (CIRMMT)
Schulich School of Music, McGill University
Montreal, Canada
Email: avrum@music.mcgill.ca

***Abstract*— An opto-acoustic cello has been designed to investigate the neural correlates of cello performance using functional magnetic resonance imaging (MRI). Through the design of specialized optical sensors, for the first time, we are able to synchronously capture a cellist's acoustic performance and musical gestures within the MRI scanner. The electromagnetic constraints and confined space of the scanner were overcome through the design of a minimalist composite cello body, a bridge and transparent fingerboard embedded with optical fibers, and a sensorized shortened bow. Using an array of fibers embedded in the fingerboard, we captured finger position and vibrato. Bending losses in fibers placed between the bridge and string, as a contact microphone, allowed us to capture the acoustic performance. Bow displacement was acquired separately using an optical flow sensor and by measuring Faraday rotation in an optical crystal within the magnetic field of the scanner.**

I. Introduction

Increasingly, neuroscientists are making use of functional MRI to correlate brain activity with behavior. The MRI scanner, with its high intensity static magnetic field, switched spatial gradient fields, and sensitive radio frequency coils present a formidable challenge to studying music performance and the brain. Optical sensing was selected for capturing performance gestures in the MRI scanner in order to ensure safety and compatibility. Previously, we have studied pianists performing in the MRI scanner [1] with an optically-sensed keyboard [2], capturing which keys are pressed and when. A cello, in contrast, allows us to investigate on-line control of continuous parameters, such as pitch and amplitude. An MRI-compatible composite fiberglass cello, without the usual resonating cavity, was designed along with several sensors to acquire musical gestures, as seen in Fig. 1.

Fig. 1. Cellist and cello in MRI scanner.

II. Sensors

A. Cello fingerboard

A transparent fingerboard embedded with pairs of emitting and receiving plastic optical fibers (POF) spaced at regular intervals enabled the direct measurement of finger position. The finger and string reflect a greater proportion of light into the receiving fiber when in contact with the fingerboard. Two different fabrication approaches were employed: casting the fingerboard in a transparent plastic resin using an aluminium mold and 3D-printing a fingerboard directly from a computer-aided design (CAD), as shown in Fig. 2. The cast resin fingerboard had high transparency and was index-matched to the refractive index of the POF. The manufacturing, however, was complicated by the need to embed all of the POF at once and ensure their placement within the mold during curing. The 3D-printed fingerboard had reduced transparency, though the CAD model included many POF mounting points, which allowed potting only the POF that were needed for a given neuroimaging study.

B. Opto-acoustic string sensors

Two different approaches to capturing the acoustic cello performance were implemented: a contact pickup based on POF bending losses and a non-contact transmission mode string displacement sensor. Each type of sensor was designed as part of a 3D-printed cello bridge, and was replicated across all four strings. The contact pickup was made from a tightly coiled length of POF inserted in a groove in the specially-designed bridge, over which a gut cello string was tensioned. Small displacements of the string during cello performance caused a proportional modulation in bending losses, allowing the acquisition of the acoustic performance, as well as the downward string pressure.

For the non-contact pickup, another 3D-printed bridge was designed to accommodate a pair of optical fibers and lenses mounted perpendicular to the string as shown in Fig. 3. The receiver and emitter fibers were aligned with the string, slightly off-center, which allowed the shadow cast by the string onto the receiver fiber to follow a monotonic response throughout

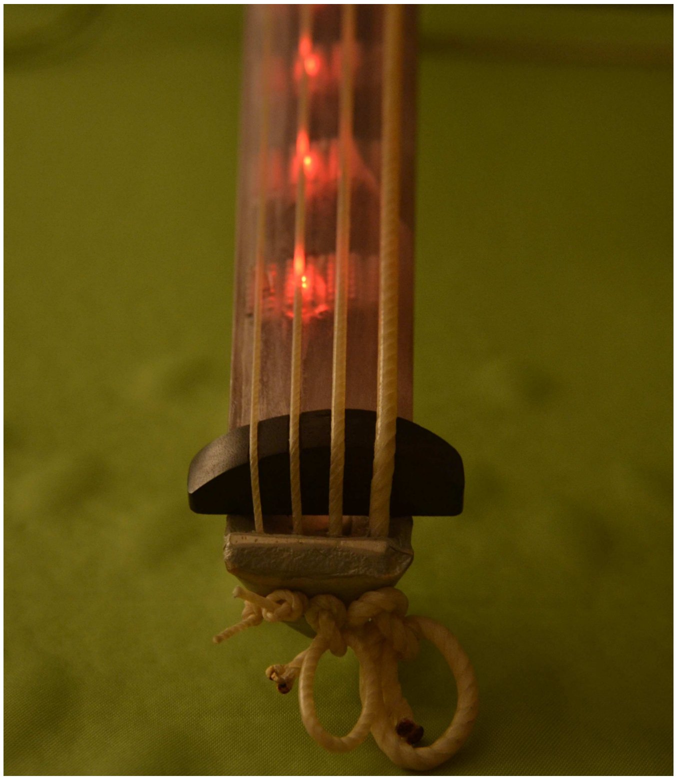

Fig. 2. 3D-printed cello fingerboard with embedded fiber optic sensors.

its usual displacement during bowed performance. The slight displacement of the string near its fixed point at the bridge caused a proportional modulation in received light intensity, thus capturing the vibration of the string.

C. Bow sensors

Cello bow sensors were designed using several different techniques: optical flow, Faraday effect, and fiber bending losses. The three different sensors provided complementary information about bow position, displacement, and velocity. We remotely measured bow movement using a multi-core POF mounted on the bridge and focused on an emitting fiber mounted on the bow, with the opposite end of the receiving fiber focused onto a commercial optical flow sensor. The flow sensor, marketed for use in a computer mouse, was configured through its serial peripheral interface (SPI) to maximize its sensitivity, resolution, and frame rate while the movement detection threshold was minimized. As the light source was moved with respect to the flow sensor, the flow sensor reported two-dimensional displacement data, representing transverse bowing gestures and changes in bow-bridge distance.

Bow movement was also captured inside the MRI scanner by measuring the Faraday effect through a 1 cm-long terbium gallium garnet (TGG) (Fig. 4). The 3D-printed sensor mount accommodated emitter and receiver fibers, and the TGG crystal sandwiched between linear polarizers and lenses, similar to [3]. Three such sensors were mounted on the bow orthogonal to each other, allowing for the three-dimensional measurement

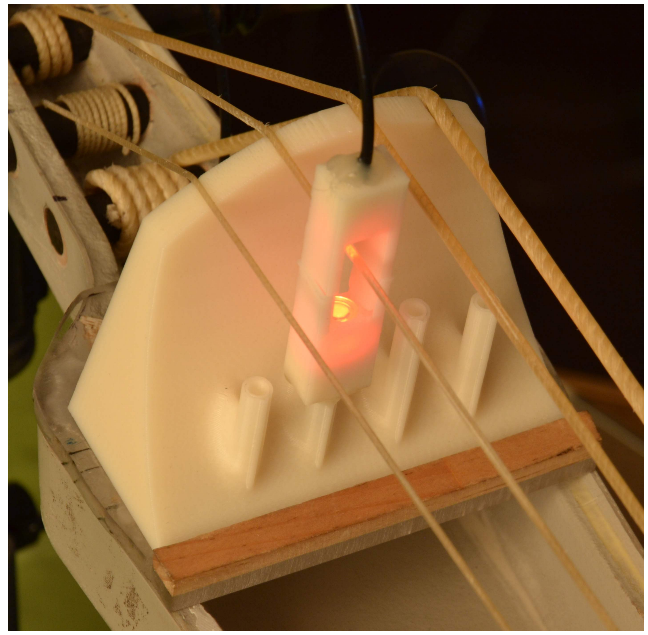

Fig. 3. 3D-printed cello bridge with integrated non-contact string sensor.

of local magnetic field. The static magnetic field at the opening of the bore, at about arm's length from the iso-center, affords a high spatial variation in transverse magnetic field, along the direction of bowing, enabling the capture of cello bowing gestures with great sensitivity.

A third bow sensor enabled the estimation of the point on the bow where it contacted the string, through pressure measurements at each end of the bow (called the frog and tip) as shown in Fig. 5. A coil of POF embedded in a silicone toroid was cast in a 3D-printed mold. As the sensor was compressed, bending losses increased, thus decreasing the received light intensity. Two such sensors, mounted at the frog and the tip between the bow hair and stick, measured the deflection of the bow hair as bow pressure was applied to the string. The sum of both sensors provided a measure of total bow pressure, itself an interesting performance parameter [4], while the difference of normalized frog and tip bow pressures provided an estimate of bow-string contact position as the bow was drawn across the string.

III. Opto-electronic acquisition system

A modular acquisition system was designed with on-board LEDs (λ = 660 nm) and photodiodes to interrogate POF sensors. It is a redesigned and more powerful version of the system described in [5]. The acquisition system was comprised of custom-designed modular circuit boards (Fig. 6) that contained the opto-electronic components, an ARM-based programmable system-on-chip (Cypress PSoC 5) with reprogrammable analog and digital blocks, SPI-programmable potentiometers, micro-SD card slot, mini-USB connector, multiple power regulators, and GPIO brought out to header pins. Each board functioned on its own as a 4-channel acquisition board connected to a PC over USB as a serial emulation, HID,

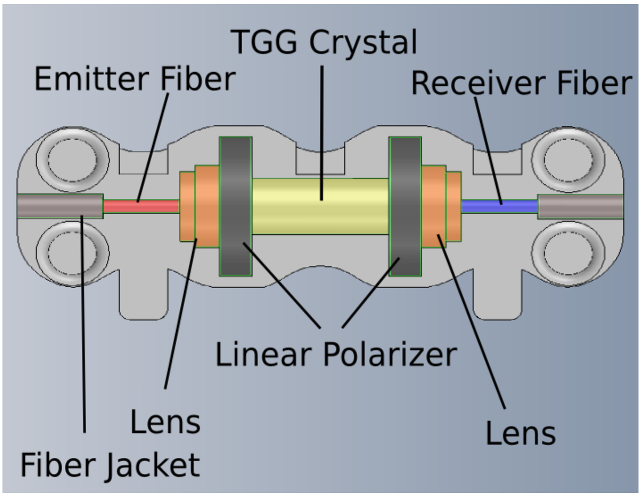

Fig. 4. Schematic of Faraday rotator: optical magnetic field sensor with terbium gallium garnet (TGG) crystal.

Fig. 5. Diminutive cello bow with silicone pressure sensors embedded with optical fibers.

MIDI, or audio device; or several boards were daisy-chained using SPI and controlled by a single-board GNU/Linux computer (e.g., the Raspberry Pi [6]). Importantly for the electromagnetically noisy MR environment, the SPI communication was made more robust with the addition of forward error-correcting codes (i.e. Reed-Solomon encoding). While the delta-sigma analog-to-digital converters on the PSoC operated at above 10 kHz (in 16-bit mode), throughput over SPI was limited to around 1 kHz per channel, per board with six boards connected.

IV. Results

All sensors were tested outside of the scanner and a subset of sensors consisting of the 3D-printed fingerboard, the non-contact string sensor, the 3D Faraday rotator, and bow pressure sensors were tested inside the MRI scanner with a cellist. These sensors were selected for their increased robustness.

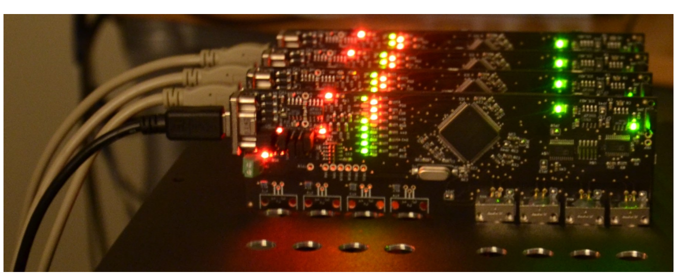

Fig. 6. An array of modular opto-electronic acquisition boards, relegated to the control room outside of the scanner.

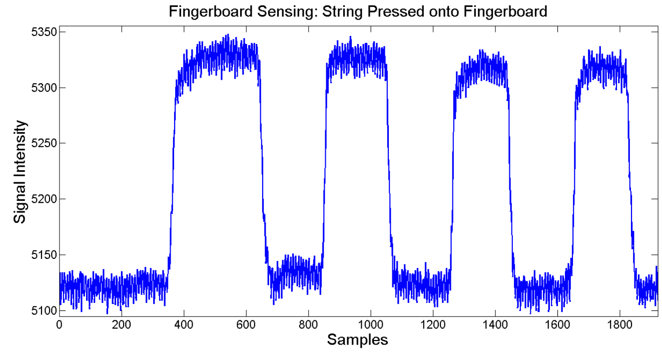

Fig. 7. Finger and string pressed against fingerboard, repeated four times (500 Hz sampling rate).

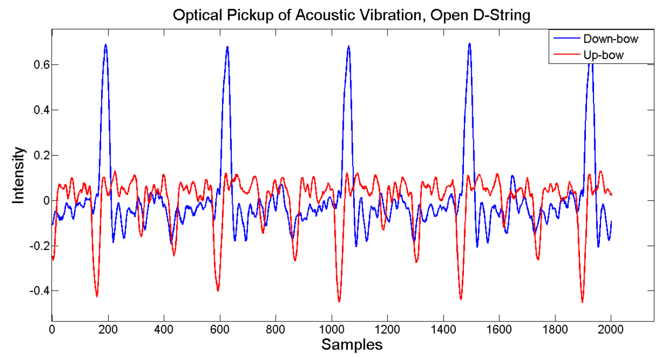

Fig. 8. Contact optical bridge pickup, up- and down-bowing of open D-string (recorded at 24-bit, 48kHz, with a professional audio recorder).

Sensor data was acquired using the opto-electronic acquisition system connected to a PC over USB, with a reporting rate of about 500 Hz. Audio-rate data was acquired with a professional portable recorder at 24-bit, 48 kHz. No image artifacts were encountered as a result of the cello and sensors, and the opto-electronic acquisition system was unaffected by the MRI acquisition sequence. All sensors performed with an adequate signal-to-noise ratio, allowing the extraction of performance gestures.

Fig. 7 shows repeated left-hand depression and release of the D-string, as sensed by a single sensor within the fingerboard. Using multiple sensors, vibrato and inter-sensor finger-string contact position along the fingerboard was resolved. Fig. 8 shows the response of the contact fiber optic pickup, while Fig. 9 shows the response of the non-contact optical pickup. Fig. 10 shows the displacement of the bow captured with the optical flow sensor. Fig. 11 shows a synchronous trace of the non-contact string sensor (A), along with the bowing gestures collected using both the three-dimensional magnetic field sensor (B), and bow pressure sensors (E). Fig. 11 (C) shows the first principal component calculated through principal component analysis. Fig. 11 (D) shows the estimated contact position of the string measured with respect to the bow between the frog and tip. The solid traces of Fig. 11 (E) show the pressure at the frog (cyan) and tip (green) while the dotted trace represents the total bow pressure.

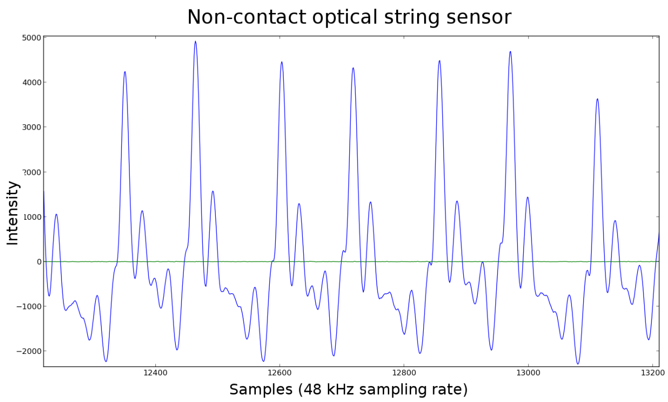

Fig. 9. Non-contact bridge pickup, down-bow on the D-string with a fundamental frequency of 176 Hz (recorded at 24-bit, 48kHz, with a professional audio recorder).

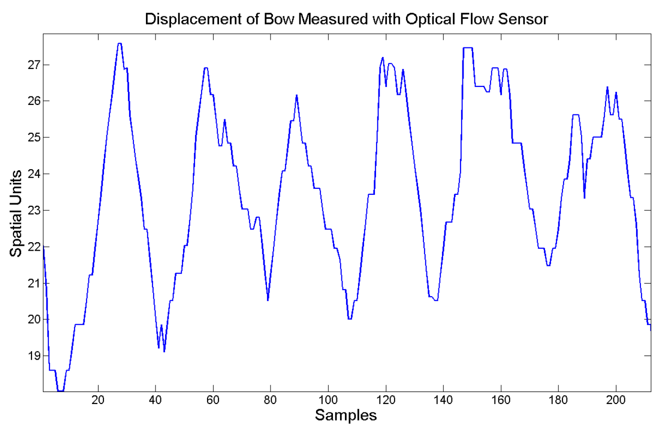

Fig. 10. Repeated bowing gesture acquired with multi-core fiber optic cable and commercial optical flow sensor (30 Hz sampling rate).

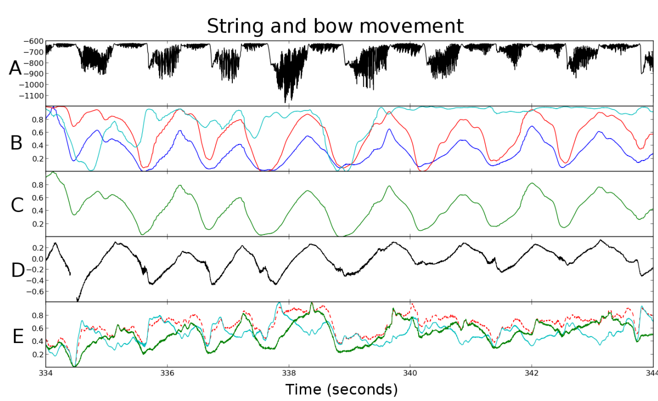

Fig. 11. Synchronous trace of a cellist performing a repeated bowing gesture in MRI scanner: (A) string vibration using non-contact optical pickup, (B) three orthogonal magnetic field components measured using 3D Faraday rotation sensor, (C) principal component of magnetic field sensors, (D) estimated bow-string contact position calculated between frog and tip, (E) frog (cyan), tip (green), and total (dashed) bow pressure measured using two coils of plastic optical fiber embedded in silicone.

V. Conclusion

We have demonstrated an MRI-compatible opto-acoustic cello that enabled electronic capture of string vibration as well as left-hand fingering and right-hand bowing gestures. The fiberglass cello contained no metal parts and sensing was accomplished using plastic optical fiber in a variety of configurations: a cello fingerboard embedded with finger-string-fingerboard proximity sensors; bridge pickups using (1) bending losses in a fiber, and (2) the modulation of transmitted light past a string; bow sensors using (1) multi-core POF with a commercial optical flow sensor that measured the relative displacement of the bow, (2) a three-dimensional Faraday rotator that measured the local magnetic field intensity within the MRI scanner correlated with absolute bow position, and (3) a pair of bow pressure sensors mounted at the tip and frog that allowed for the estimation of bow-string contact position. A modular opto-electronic acquisition system was also presented along with measurements of cello performance gestures. In addition to its engineering significance, the novel musical instrument design, the MRI-compatible fiber optic sensors, and the acquisition system are each a significant contribution to the field of neuroscience and music. A functional MRI study is underway to better understand the neural substrates underlying auditory-motor integration in cellists [7].

Acknowledgment

Thanks to Melanie Segado, Virginia Penhune, and Robert Zatorre for this wonderful collaboration. Thanks as well to Anthony Piciacchia and Steven Phillips for help with mechanical design and fabrication. Thanks to Yves Méthot, Harold Kilianski, Julien Boissinot, and other CIRMMT staff members for their technical assistance. Thanks to Richard Benoit and Éric Gagné of Wilder and Davis Luthiers for your advice and handiwork. Thanks to IDMIL members Mark Zadel, Stephen Sinclair, Joseph Malloch, and Joseph Thibodeau. Funding provided by CIRMMT and the Canada Foundation for Innovation.

References

[1] R. M. Brown, J. L. Chen, A. Hollinger, V. B. Penhune, C. Palmer, and R. J. Zatorre, "Repetition suppression in auditory-motor regions to pitch and temporal structure in music," *Journal of Cognitive Neuroscience*, vol. 25, no. 2, pp. 313–328, Nov. 2012.

[2] A. Hollinger, "Design of fMRI-compatible electronic musical interfaces," Master's Thesis, McGill University, 2008.

[3] M. Bock, R. Umathum, J. Sikora, S. Brenner, E. N. Aguor, and W. Semmler, "A Faraday effect position sensor for interventional magnetic resonance imaging," *Physics in Medicine and Biology*, vol. 51, no. 4, pp. 999–1009, Feb. 2006.

[4] E. Schoonderwaldt, "Mechanics and acoustics of violin bowing: Freedom, constraints and control in performance," Ph.D. dissertation, KTH, 2009.

[5] A. Hollinger and M. M. Wanderley, "Optoelectronic acquisition and control board for musical applications," in *Proceedings of the International Conference on New Interfaces for Musical Expression (NIME)*, G. Essl, B. Gillespie, M. Gurevich, and S. O'Modhrain, Eds. Ann Arbor, Michigan: University of Michigan, May 21-23 2012.

[6] (2013) The Raspberry Pi Foundation website. [Online]. Available: http://www.raspberrypi.org/

[7] M. Segado, A. Hollinger, V. B. Penhune, and R. J. Zatorre, "Auditory-motor integration in cellists," in *Proceedings of the biennial meeting of the Society for Music Perception and Cognition (SMPC)*, 2013.